Fossil bryophytes as recorders of ancient CO_2 levels: Experimental evidence and a Cretaceous case study

Benjamin J. Fletcher, David J. Beerling, and Stuart J. Brentnall
Department of Animal and Plant Sciences, University of Sheffield, Sheffield, UK

Dana L. Royer[1]
Department of Geosciences, Pennsylvania State University, University Park, Pennsylvania, USA

Received 23 February 2005; revised 9 June 2005; accepted 16 June 2005; published 19 August 2005.

[1] Biological and geochemical CO_2 proxies provide critical constraints on understanding the role of atmospheric CO_2 in driving climate change during Earth history. As no single existing CO_2 proxy is without its limitations, there is a clear need for new approaches to reconstructing past CO_2 concentrations. Here we develop a new pre-Quaternary CO_2 proxy based on the stable carbon isotope composition ($\delta^{13}C$) of astomatous land plants. In a series of CO_2-controlled laboratory experiments, we show that the carbon isotope discrimination ($\Delta^{13}C$) of a range of bryophyte (liverwort and moss) species increases with atmospheric CO_2 across the range 375 to 6000 ppm. Separate experiments establish that variations in growth temperature, water content and substrate type have minor impacts on the $\Delta^{13}C$ of liverworts but not mosses, indicating the greater potential of liverworts to faithfully record past variations in CO_2. A mechanistic model for calculating past CO_2 concentrations from bryophyte $\Delta^{13}C$ (White et al., 1994) is extended and calibrated using our experimental results. The potential for fossil liverworts to record past CO_2 changes is investigated by analyzing the $\delta^{13}C$ of specimens collected from Alexander Island, Antarctica dating to the "greenhouse" world of the mid-Cretaceous. Our analysis and isotopic model yield mid-Cretaceous CO_2 concentrations of 1000–1400 ppm, in general agreement with independent proxy data and long-term carbon cycle models. The exceptionally long evolutionary history of bryophytes offers the possibility of reconstructing CO_2 concentrations back to the mid-Ordovician, pre-dating all currently used quantitative CO_2 proxies.

Citation: Fletcher, B. J., D. J. Beerling, S. J. Brentnall, and D. L. Royer (2005), Fossil bryophytes as recorders of ancient CO_2 levels: Experimental evidence and a Cretaceous case study, *Global Biogeochem. Cycles*, *19*, GB3012, doi:10.1029/2005GB002495.

1. Introduction

[2] Atmospheric CO_2 is an important greenhouse gas and is widely regarded as the primary driver of climate changes over the Phanerozoic (past 540 million years) [*Crowley and Berner*, 2001; *Royer et al.*, 2004], although this view has been challenged [*Veizer et al.*, 2000]. Nevertheless, our understanding of Earth's Phanerozoic CO_2 history is largely based on models of the long-term carbon cycle simulating atmospheric CO_2 changes due to the imbalance between its supply from volcanoes and metamorphic degassing and removal by silicate rock weathering [*Tajika*, 1998; *Berner and Kothavala*, 2001; *Wallmann*, 2001; *Kashiwagi and Shikazono*, 2003; *Berner*, 2004; *Bergman et al.*, 2004]. All such models are crucially dependent upon proxy estimates of past CO_2 concentrations for assessment of their performance and reliability [*Royer et al.*, 2001a; *Beerling and Royer*, 2002].

[3] There are currently four main proxies for determining pre-Quaternary atmospheric CO_2 concentrations: the $\delta^{13}C$ of pedogenic minerals, either carbonate [*Cerling*, 1991] or goethite [*Yapp and Poths*, 1992]; the $\delta^{13}C$ of phytoplankton [*Freeman and Hayes*, 1992; *Pagani et al.*, 1999]; vascular plant stomatal density and index [*Van der Burgh et al.*, 1993; *McElwain and Chaloner*, 1995; *Royer et al.*, 2001a, 2001bb; *Beerling and Royer*, 2002], and the $\delta^{11}B$ of fossilized calcium carbonate shells of planktonic foraminifera [*Pearson and Palmer*, 2000]. Each of these proxies has limitations in their capacity to faithfully reconstruct past CO_2 concentrations [*Royer et al.*, 2001a]. For example, the pedogenic carbonate method has large error terms in comparison with other proxies, especially at low CO_2, the $\delta^{13}C$ of phytoplankton is sensitive to factors such as cell geometry, growth rate, and the presence of carbon-concentrating mechanisms (CCMs) [*Laws et al.*, 2002; *Giordano et al.*, 2005], the stomatal index approach has reduced sensitivity

[1] Now at Department of Earth and Environmental Sciences, Wesleyan University, Middletown, Connecticut, USA.

0886-6236/05/2005GB002495$12.00

to high atmospheric CO_2 concentrations, and the boron isotope method requires the effects of the total alkalinity of the oceans to be removed and a control on the $\delta^{11}B$ of the ocean. These difficulties indicate the clear need for new approaches to better achieve a proxy-based Phanerozoic CO_2 history of the Earth.

[4] The potential for developing a new terrestrial pre-Quaternary CO_2 proxy emerges from theoretical studies on the environmental controls on bryophyte carbon isotope fractionation ($\Delta^{13}C$) during photosynthesis [*White et al.*, 1994; *Figge and White*, 1995]. Unlike vascular plants, bryophytes (liverworts, hornworts and mosses) lack stomata or thick cuticles in the dominant gametophyte stage of the life cycle [*Raven et al.*, 1999]. Some liverwort species possess fixed aperture pores and internal air spaces to enhance diffusion and photosynthetic carbon assimilation [*Raven*, 2002]. Photosynthetic CO_2 uptake and $\Delta^{13}C$ by bryophytes occur by passive diffusion of CO_2 into the cells and depend on the kinetics of the primary carboxylating enzyme ribulose-1,5-carboxylase/oxygenase (Rubisco), both of which respond to the concentration of atmospheric CO_2. The only exception is some hornwort species which possess CCMs [*Smith and Griffiths*, 2000]. Because of their comparatively simple structure, bryophyte $\Delta^{13}C$ is analogous to that of phytoplankton which, in the absence of CCMs, is primarily controlled by the uptake of CO_2 dissolved in seawater, and hence the atmospheric concentration [*Laws et al.*, 1995; *Popp et al.*, 1998; *Laws et al.*, 2002; *Giordano et al.*, 2005]. As a result, bryophyte $\Delta^{13}C$ provided a basis for reconstructing late Quaternary atmospheric CO_2 concentrations from $\delta^{13}C$ analyses of southern South American peat cores [*White et al.*, 1994; *Figge and White*, 1995]. However, the presumed sensitivity of bryophyte $\Delta^{13}C$ to CO_2 has not yet been investigated with controlled environment laboratory experiments.

[5] Here we report a series of detailed laboratory investigations, field surveys and analyses of fossil materials designed to establish the basis for fossil bryophytes as a new pre-Quaternary CO_2 proxy based on their photosynthetic $\Delta^{13}C$ behavior. We performed a suite of controlled environment experiments with a range of liverwort and moss species (including thallose liverworts with and without pores) to determine their $\Delta^{13}C$ responses to different growth CO_2 concentrations. In a separate series of studies, we quantified four potentially important sources of natural variation in $\Delta^{13}C$ by examining the effect of warming (by + 4°C), water availability and substrate type and, for thallose liverworts, spatial heterogeneity along the thallus, to determine the potential of each factor to mask a CO_2 signal in the fossils. We then revisit the isotopic model of *White et al.* [1994] linking $\Delta^{13}C$ and CO_2 to formulate a mechanistic version calibrated against our experimental results. Our aim is to produce a model capturing the physiological responses of bryophytes to CO_2 for robust reconstructions of past atmospheric CO_2 concentrations from $\Delta^{13}C$ values.

[6] In the final section, we describe a detailed case study of the isotopic fractionation exhibited by fossil liverworts from Antarctica dating to the start of the Cretaceous greenhouse interval (Albian). Fossil materials of this age provide an interesting test case for the new CO_2 proxy because multiple biotic and geochemical climate indices show Earth experienced a warm largely ice-free climate with a reduced pole-to-equator temperature gradient [*Macleod et al.*, 2000], conditions widely attributed to a CO_2-rich atmosphere [*Beerling and Royer*, 2002; *Royer et al.*, 2004].

2. Materials and Methods

2.1. CO_2 Controlled Laboratory Growth Experiments

[7] We propagated two species of liverwort (*Lunularia cruciata* (L.) Dum. ex Lindb. and *Marchantia polymorpha* L.) and moss (*Funaria hygrometrica* Hedw. and *Leptobryum pyriforme* (Hedw.) Wils.) from gemmae and spores, respectively, collected from the University of Sheffield Tapton Experimental Gardens. Spores or gemmae were sown on sand in pots of a moist 3:2 mix of sand and vermiculite containing 5 mL slow release fertilizer (Osmocote, Scotts, Ipswich, U.K.), and sprayed weekly with systemic fungicide (Fungus fighter, pbi Home & Garden Ltd., Hertfordshire, U.K.).

[8] Plants were grown in replicated 4-L Perspex growth chambers ($n = 5$ per CO_2 concentration), each supplied with pressure-regulated compressed air mixed with CO_2 (BOC gases, Surrey, U.K.) by a mass-flow controller as described previously [*Beerling et al.*, 1998], to provide a range of target CO_2 concentrations between near-present-day values (375 ppm) to very high values (~6000 ppm). Needle valves regulated a 750 ± 50 mL min^{-1} air supply to each chamber which was filtered through $KMnO_4$ to remove volatile organic compounds and humidified to 60 ± 10% relative humidity, with water vapor and CO_2 concentrations measured using an infra-red gas analyzer (Ciras-1 IRGA, PP systems, Herts, U.K.). The chambers were housed in a pair of controlled environment cabinets (Conviron, Winnipeg, Canada) providing 180 ± 10 μmol light m^{-2} s^{-1} for 12 hours per day, at 22°C (day) and 19°C (night) (PAR sensor, Skye Instruments, Powys, U.K.; Squirrel data logger, Grant Instruments, Cambridgeshire, U.K.). The experimental set-up was run twice, each time for a duration of 6 weeks, with an ambient CO_2 control and two elevated CO_2 treatments (Table 1).

[9] Two additional experiments were also performed using plant growth cabinets to expose brophytes to current ambient (375−387 ppm) and elevated CO_2 concentrations (797 ppm and 1624 ppm). Conditions for these experiments were as described above, except the plants were grown on four replicate pots of moist compost at a constant day-night temperature of 20°C. In the first experiment using this system, the same species as above were grown at 375 and 797 ppm. In the second experiment, a liverwort species without pores, *P. endiviifolia* (Dicks.) Dum., was transplanted from natural field populations in Sheffield, U.K. (Wisewood Weir, River Loxley, Sheffield, South Yorkshire, U.K.), and grown at 387 and 1624 ppm CO_2.

2.2. Growth Temperature and Substrate Experiments

[10] To examine the possible influence of substrate type and growth temperature on $\Delta^{13}C$ variation at a constant atmospheric CO_2 concentration, we cultivated four species of liverworts on sandy (3:2 sand:vermiculite mixture) and

Table 1. Carbon Isotope Composition of Bryophyte Species and Source CO_2 From the CO_2 Experiments

$[CO_2]_a$	Species	Group	$\delta^{13}C_a$, ‰	n	$\delta^{13}C_p$, ‰	$\Delta^{13}C$, ‰
375	*Funaria hygrometrica*	moss	−11.3	4	−23.35 ± 0.17	12.31 ± 0.18
	Leptobryum pyriforme	moss	−11.3	4	−21.66 ± 0.40	10.56 ± 0.42
	Lunularia cruciata	liverwort	−11.3	4	−27.04 ± 0.70	16.14 ± 0.73
	Marchantia polymorpha	liverwort	−11.3	4	−29.77 ± 0.13	19.01 ± 0.13
797	*F. hygrometrica*	moss	−23.3	4	−44.57 ± 0.15	22.31 ± 0.16
	L. pyriforme	moss	−23.3	4	−38.25 ± 0.33	15.60 ± 0.35
	L. cruciata	liverwort	−23.3	4	−44.98 ± 0.53	22.75 ± 0.57
	M. polymorpha	liverwort	−23.3	4	−45.81 ± 0.12	23.64 ± 0.13
402	*F. hygrometrica*	moss	−10.1	4	−26.76 ± 0.38	16.85 ± 0.40
	L. pyriforme	moss	−10.1	1	−21.48	11.63
	L. cruciata	liverwort	−10.1	5	−29.09 ± 0.60	19.56 ± 0.63
	M. polymorpha	liverwort	−10.1	5	−29.55 ± 0.51	20.04 ± 0.54
1318	*F. hygrometrica*	moss	−26.7	3	−48.57 ± 0.40	22.94 ± 0.43
	L. pyriforme	moss	−26.7	1	−45.92	20.09
	L. cruciata	liverwort	−26.7	5	−50.00 ± 0.19	24.48 ± 0.21
	M. polymorpha	liverwort	−26.7	5	−49.70 ± 0.35	24.15 ± 0.38
3011	*F. hygrometrica*	moss	−30.2	2	−56.52 ± 0.43	27.86 ± 0.47
	L. pyriforme	moss	−30.2	1	−56.35	27.67
	L. cruciata	liverwort	−30.2	5	−55.40 ± 0.67	26.64 ± 0.73
	M. polymorpha	liverwort	−30.2	5	−55.07 ± 0.22	26.28 ± 0.24
383	*L. cruciata*	liverwort	−12.2	5	−27.83 ± 0.4	16.05 ± 0.42
	M. polymorpha	liverwort	−12.2	5	−29.67 ± 0.25	17.98 ± 0.26
2202	*L. cruciata*	liverwort	−30.4	5	−54.60 ± 0.47	25.56 ± 0.51
	M. polymorpha	liverwort	−30.4	5	−54.28 ± 0.6	25.21 ± 0.65
6008	*L. cruciata*	liverwort	−33.6	5	−59.31 ± 0.97	27.37 ± 1.06
	M. polymorpha	liverwort	−33.6	5	−58.02 ± 0.83	25.96 ± 0.91
387	*Pellia endiviifolia*	liverwort	−12.2	5	−26.37 ± 0.29	14.59 ± 0.30
1624	*P. endiviifolia*	liverwort	−29.2	5	−51.24 ± 0.22	23.23 ± 0.24

peaty (potting compost) moist substrates in warm or cool conditions in a factorial experimental design. *Conocephalum conicum* (L.) Lindb. and *Pellia epiphylla* L. Corda were transplanted from natural field populations in Sheffield, U.K. (River Rivelin, Under Tofts, Sheffield, South Yorkshire, U.K. and River Loxley, Acorn Hill, Sheffield, South Yorkshire, U.K.), and *L. cruciata* and *M. polymorpha* propagated as before. Three replicate pots per species were cultivated in shaded, well-ventilated indoor greenhouse locations at the University of Sheffield Tapton Experimental Gardens experiencing either ambient temperatures or ambient temperatures with +4 °C warming. Maximum and minimum temperatures recorded during the experiment were 13/33°C and 9/29°C for the warm and cool treatments, respectively; light and humidity levels varied by <10%. Newly developed plant material from each pot was harvested after 6 weeks.

2.3. Field Survey of Water Availability Effects on Bryophyte $\Delta^{13}C$

[11] We collected bulk tissues of three species of liverworts and mosses from naturally occurring field popula-

Table 2. Discrimination Against ^{13}C by Bryophytes in Wet and Dry Habitats[a]

Species	Group	Site Description	Water Content/Dry Weight, g	$\Delta^{13}C$, ‰
Conocephalum conicum	liverwort	leaking mill race wall	26.87 ± 3.09	20.18 ± 0.55
		dry mill race wall	20.50 ± 3.19	20.14 ± 0.38
		wet site–dry site	**6.37**	**0.04**
Hyocomium amoricum	moss	leaking mill race wall	23.95 ± 2.56	19.79 ± 0.42
		dry mill race wall	2.98 ± 1.11	18.91 ± 0.25
		wet site–dry site	**20.97**	**0.88**
Lunularia cruciata	liverwort	wet ditch bank	16.89 ± 1.65	22.71 ± 0.5
		dry ditch bank	8.27 ± 0.35	22.2 ± 0.23
		wet site–dry site	**8.62**	**0.51**
Eurhynchium praelongum	moss	wet ditch bank	8.10 ± 0.93	19.05 ± 0.39
		dry ditch bank	3.56 ± 0.50	18.11 ± 0.38
		wet site–dry site	**4.54**	**0.94**
Pellia endiviifolia	liverwort	under dripping cliff	13.32 ± 1.03	17.58 ± 0.66
		dry cliff–side	11.95 ± 0.59	17.02 ± 0.29
		wet site–dry site	**1.37**	**0.56**
Mnium hornum	moss	under dripping cliff	10.36 ± 1.05	18.86 ± 0.22
		dry cliff–side	1.43 ± 0.16	14.57 ± 0.29
		wet site–dry site	**8.93**	**4.28**

[a]Data are ± standard error.

Table 3. Cretaceous $[CO_2]_a$ Predictions From the Stable Carbon Isotope Composition of Fossil Liverworts From Alexander Island, Antarctica[a]

Species	BAS Specimen ID (Number of Measurements)	Geological Stage	Age, Mya	Locality	$\delta^{13}C_{fossil}$, ‰	$\delta^{13}C_p$, ‰	$\delta^{13}C_{atm}$, ‰	$\Delta^{13}C$, ‰	Predicted $[CO_2]_a$, ppm
Marchantites	KG.4737.2	Late Albian	99.6–106.4	Citadel Bastion	−27.03	−28.88	−5.60	23.97	1391
arcuatus	KG.4737.3 (n = 2)	Late Albian	99.6–106.4	Citadel Bastion	−25.82 ± 0.00	−27.67	−5.60	22.70	925
	average				**−26.43**	**−28.28**		**23.34**	**1112**
M. pinnatus	KG.4741.65	Late Albian	99.6–106.4	North Coal Nunatak	−25.64	−27.49	−5.60	22.51	882
M. rosulatus	KG.4746.1	Late Albian	99.6–106.4	North Coal Nunatak	−28.27	−30.12	−5.60	25.28	2857
	***Marchantites* average**				**−26.69**	**−28.54**	**−5.60**	**23.61**	**1514 ± 462**
Thallites	KG.4725.1	Late Albian	99.6–106.4	Citadel Bastion	−27.85	−29.70	−5.60	24.84	2105
bicostatus	KG.4725.4	Late Albian	99.6–106.4	Citadel Bastion	−26.41	−28.26	−5.60	23.32	1105
	KG.4725.12	Late Albian	99.6–106.4	Citadel Bastion	−25.87	−27.72	−5.60	22.75	937
	***Thallites* average**				**−26.71**	**−28.56**		**23.63**	**1382 ± 364**
Unspecified	KG.4747.39	Late Albian	99.6–106.4	North Coal Nunatak	−27.32	−29.17	−5.60	24.28	1580
Liverwort	KG.4737.12 (n = 2)	Late Albian	99.6–106.4	Citadel Bastion	−26.29 ± 0.11	−28.14	−5.60	23.19	1063
	KG.4737.65	Late Albian	99.6–106.4	Citadel Bastion	−26.93	−28.78	−5.60	23.86	1333
	KG.4715.19	Late Albian	99.6–106.4	Titan Nunatak	−26.16	−28.01	−5.60	23.06	1022
	KG.4671.18	Late Albian	99.6–106.4	North Coal Nunatak	−26.52	−28.37	−5.60	23.43	1146
	KG.4721.29	Late Albian	99.6–106.4	Titan Nunatak	−25.87	−27.72	−5.60	22.75	940
	KG.4737.41	Late Albian	99.6–106.4	Citadel Bastion	−26.01	−27.86	−5.60	22.90	976
	KG.4737.66 (n = 2)	Late Albian	99.6–106.4	Citadel Bastion	−25.15 ± 0.19	−27.00	−5.60	22.00	782
	unspecified average				**−26.28**	**−28.13**		**23.18**	**1105 ± 88**
	all samples				−26.48 ± 0.22	−28.34		23.40 ± 0.23	1269 ± 91

[a]Data are ± standard error. Age from *Gradstein et al.* [2004].

tions by the River Rivelin, Sheffield, South Yorkshire, U.K., in neighboring patches of contrasting moisture supply, either dry (water from rainfall only) or wet (continually splashed with water; see Table 2). The water contents and carbon isotopic composition of 10 individuals of each species at the dry and wet sites were determined by weighing before and after drying for 1 week at 65°C.

2.4. Spatial Heterogeneity in Liverwort Thallus $\delta^{13}C$

[12] We quantified the extent of variation in carbon isotopic composition along the liverwort thallus by dividing thalli of the three largest species (*C. conicum*, 6–8 cm in length; *M. polymorpha*, 3–4 cm in length; *L. cruciata*, 2–3 cm in length) across the length into equal quarters. This procedure facilitated comparison between species (and specimens) with different growth rates. The $\delta^{13}C$ was determined for each portion of thallus of five replicate individuals. *M. polymorpha* and *L. cruciata* were collected from outdoor sites at the University of Sheffield Tapton Experimental Gardens, and *C. conicum* from near the River Rivelin, Sheffield, South Yorkshire, U.K.

2.5. Age, Source, and Taxonomy of Fossil Materials

[13] Liverworts from the Triton Point Member of the Neptune Glacier Formation (Fossil Bluff Group) [*Kelly and Moncreiff*, 1992; *Moncreiff and Kelly*, 1993; *Cantrill*, 1997] were obtained from curated collections held at British Antarctic Survey, Cambridge, U.K. Paleolatitude was estimated to be ~72°S [*Smith et al.*, 1994]. In most cases, paleobotanical and sedimentary evidence indicated a riparian habitat [*Cantrill*, 1997]. Carbon was obtained from 15 Cretaceous compression fossil liverwort samples (Table 3). Some fossils belonged to the form genus *Marchantites* assigned to the basal liverwort group Marchantiopsida [*Oostendorp*, 1987; *Shaw and Renzaglia*, 2004] containing organisms with complex thalli such as the extant *Marchantia* and *Lunularia*. The *Thallites bicostatus* samples did not show evidence of complex thalli, and in this respect resembled Metzgeriidae, the group containing *Pellia*. A further group of samples assigned to the generic category of liverwort was also analyzed.

[14] Only those specimens yielding at least 15 μg C (instrumental error <0.5‰) were included in the analysis to ensure a reproducible measurement. After removal of the fossil material from the rock, the sample was treated with 30% HCl for 1 day and rinsed several times in distilled water to remove carbonates prior to $\delta^{13}C$ analysis.

2.6. Stable Carbon Isotope Analysis

[15] Stable carbon isotope measurements were made on bulk tissues of extant and fossil specimens using an ANCA GSL preparation module, coupled to a 20–20 stable isotope analyzer (PDZ Europa, Cheshire, U.K.), which was also used for analysis of air samples. Materials from the experiments and field surveys were cleaned in distilled water, dried and powdered prior to isotopic analysis. Carbon isotopic composition ($\delta^{13}C$) is expressed as $[(R_{sample}/R_{standard}) - 1] \times 1000$, where R is the $^{13}C/^{12}C$ ratio of each sample and the Peedee Belemnite standard. Plant $\Delta^{13}C$ was calculated according to [*Farquhar et al.*, 1982]

$$\Delta^{13}C = \frac{\left(\delta^{13}C_a - \delta^{13}C_p\right)}{\left(1 + \left(\delta^{13}C_p/1000\right)\right)}, \quad (1)$$

where $\delta^{13}C_a$ and $\delta^{13}C_p$ are the isotopic composition of the air and the plants, respectively. Replicate analyses

made on the same modern and fossil specimens with this instrument had a reproducibility of <0.5‰. Reproducibility within genera was generally high, within 1.2‰ of the average.

[16] For the growth chamber experiments, we calculated $\Delta^{13}C$ using $\delta^{13}C_a$ values obtained by sampling air from each CO_2 treatment four times at four points during the day when plants were actively assimilating CO_2. A simple mass balance calculation was used to provide an additional check on the $\delta^{13}C_a$ measurements, constrained by measuring the $\delta^{13}C_a$ of CO_2 in the ambient treatments and pure CO_2 from the cylinders, to give the $\delta^{13}C_a$ of CO_2 in the elevated treatments as

$$\delta^{13}C_{elevated} = \left(\frac{[CO_2]_{ambient}}{[CO_2]_{elevated}} \cdot \delta^{13}C_{ambient}\right) + \left(\frac{[CO_2]_{elevated} - [CO_2]_{ambient}}{[CO_2]_{elevated}} \cdot \delta^{13}C_{cylinder}\right). \quad (2)$$

[17] For plants collected in the field or grown in experimental gardens in 2004, atmospheric $\delta^{13}C_a$ in Sheffield was measured as −11.5‰. We estimated a $\delta^{13}C_a$ value for the mid-Cretaceous (100 Ma) of −5.6‰ (standard deviation ± 1.4‰) from the $\delta^{13}C$ records of marine calcium carbonate fossils [*Veizer et al.*, 1999]. This approach assumes that $\delta^{13}C_a$ is in long-term equilibrium with marine inorganic carbon, with an offset of −7‰ [*Mora et al.*, 1996; *Beerling et al.*, 2002] but ignores the weak temperature dependency of the system [*Mook et al.*, 1974; *Mook*, 1986]. To estimate past CO_2 concentrations from fossils it is necessary to correct for diagenetic effects on $\delta^{13}C_p$ before calculating $\Delta^{13}C$. For this purpose, we applied a −1.85‰ correction to the original fossil $\delta^{13}C_p$ values, the mean effect of two chemical treatments designed to mimic diagenetic alteration in thallose liverworts by removing non-degradation resistant material [*Fletcher et al.*, 2004].

3. Modeling Bryophyte Stable Carbon Isotope Composition

[18] According to the general, well-established mechanistic model, the isotopic composition of plants with the C_3 photosynthetic pathway (see notation section for symbols and units) can be defined by [*Farquhar et al.*, 1982]

$$\delta^{13}C_p = \delta^{13}C_a - a - (b-a)\left(\frac{[CO_2]_i}{[CO_2]_a}\right) + \frac{f\cdot\Gamma_* + e\cdot R_d/k}{[CO_2]_a}. \quad (3)$$

The term on the right-hand side of the equation exerts a minor influence on $\delta^{13}C_p$. Equation (3) therefore indicates that $\delta^{13}C_p$ depends principally on the intracellular/atmospheric $[CO_2]$ ratio ($[CO_2]_i/[CO_2]_a$), which is regulated by the photosynthetic demand for CO_2 and its supply to the mesophyll tissue from the atmosphere [*Farquhar et al.*, 1989]. Vascular plants, with a thick cuticle and stomatal pores, regulate $[CO_2]_i/[CO_2]_a$ primarily through stomatal activities which act to optimize carbon gain with respect to water loss under changing environmental conditions [*Cowan*, 1977; *Farquhar and Lloyd*, 1993]. However, because bryophytes are astomatous and unable to regulate gas exchange in this manner, their CO_2 uptake and H_2O loss is controlled by simple diffusion [*Proctor*, 1982]. $[CO_2]_i/[CO_2]_a$ depends on two things: $[CO_2]_a$, and the difference between ambient and internal CO_2 ($[CO_2]_a - [CO_2]_i$), which in bryophytes is dependant simply on the rate of CO_2 consumption by photosynthesis (A), and the total resistance to inward CO_2 diffusion (r), described by

$$[CO_2]_a - [CO_2]_i = A\cdot r. \quad (4)$$

Re-arranging equation (4) for $[CO_2]_i$ and substituting equation (4) into equation (3) gives

$$\delta^{13}C_p = \delta^{13}C_a - a - (b-a)\left(1 - \frac{r\cdot A}{[CO_2]_a}\right) + \frac{f\cdot\Gamma_* + e\cdot\frac{R_d}{((A+R_d)/([CO_2]_a - r\cdot A - \Gamma_*))}}{[CO_2]_a}, \quad (5)$$

which provides a reasonably complete description of the main physical and biological factors influencing bryophyte $\delta^{13}C$.

[19] However, after substituting in known values (notation section), equation (5) contains two unknown terms, A and r, preventing its use for estimating $[CO_2]_a$. As $(r\cdot A)$ has units of μmol mol^{-1} (ppm) and is equivalent to $([CO_2]_a - [CO_2]_i)$, we address this issue by solving equation (4) for the term $([CO_2]_a - [CO_2]_i)$,

$$([CO_2]_a - [CO_2]_i) = \frac{[CO_2]_a\cdot\left(\delta^{13}C_p - \delta^{13}C_a + b - g\right) - (f-g)\cdot\Gamma_*}{b-a-g}. \quad (6)$$

In mosses, experimental observations indicate A increases almost linearly with $[CO_2]_a$ up to around 800 ppm [*Silvola*, 1985; *Williams and Flanagan*, 1998]; in liverworts A increases linearly up to around 400 ppm in some but not all species [*Smith and Griffiths*, 2000; *Griffiths et al.*, 2004]. A linear response of A, assuming a constant r, implies $(r\cdot A)$, and hence $([CO_2]_a - [CO_2]_i)$, is also a linear function of $[CO_2]_a$. We determined the response of $([CO_2]_a - [CO_2]_i)$ to $[CO_2]_a$ from our laboratory experiments using equation (6) and a simple linear fit of the form

$$\left([CO_2]_a - [CO_2]_i\right)_{fit} = m\cdot[CO_2]_a + c, \quad (7)$$

without measuring long-term r or A responses individually. By substituting $(m\ [CO_2]_a + c)$ for $([CO_2]_a - [CO_2]_i)$ into equation (6), we obtain by rearrangement an expression for predicting the $[CO_2]_a$ from any given pair of bryophyte $\delta^{13}C$ and $\delta^{13}C_a$ values,

$$[CO_2]_a = \frac{-\left([f-g]\cdot\Gamma_*\right)/(b-a-g) - c}{m - \left(\delta^{13}C_p - \delta^{13}C_a + b - g\right)/(b-a-g)}. \quad (8)$$

Conversely, it is also possible to predict bryophyte $\delta^{13}C$ from known $\delta^{13}C_a$ and $[CO_2]_a$ values by rearrangement of equation (8),

$$\delta^{13}C_p = \frac{(b-a-g)\cdot\left(m\cdot[CO_2]_a + c\right) + (f-g)\cdot\Gamma_*}{[CO_2]_a} + \delta^{13}C_a - b - g. \quad (9)$$

4. Results and Discussion

4.1. Experimentally Determined Response of $\Delta^{13}C$ to Atmospheric CO_2

[20] In the experiments, whole-tissue bryophyte $\delta^{13}C$ became more negative with increasing $[CO_2]_a$ (Figure 1, top). This partly reflects changes in the $\delta^{13}C$ of the assimilated CO_2, which also became more negative with the addition of increasing amounts of fossil fuel-derived CO_2 (Figure 1, middle). However, biological processes amplified the change in $\delta^{13}C_p$ relative to $\delta^{13}C_a$, as shown by the increase in $\Delta^{13}C$ with $[CO_2]_a$ (Figure 1, bottom). Liverwort $\Delta^{13}C$ increased markedly as $[CO_2]_a$ rose between 400 ppm and 800 ppm, and continued to increase toward an asymptote above ~6000 ppm (Table 1). Moss $\Delta^{13}C$ responded to CO_2 similarly, but was more variable between the different species studied (Table 1). Atmospheric CO_2 exerted a similar impact on the $\Delta^{13}C$ of *P. endiviifolia*, a liverwort without pores, although there was an offset suggesting a possible increased diffusion resistance limiting photosynthesis (Table 1).

[21] The pattern of $\Delta^{13}C$ response to $[CO_2]_a$ seen in bryophytes is consistent with astomatous photosynthetic CO_2 uptake exhibited by marine phytoplankton and on which the alkenone CO_2 proxy is based, but without the possible complications of CCM's [*Laws et al.*, 1995; *Popp et al.*, 1998; *Laws et al.*, 2002; *Giordano et al.*, 2005]. The response in bryophytes is brought about because with rising CO_2, the $[CO_2]_i/[CO_2]_a$ ratio tends toward 1 and discrimination tends toward 30‰ [*Farquhar et al.*, 1989], as the preferential selection of ^{12}C by Rubisco during photosynthetic CO_2 fixation is enhanced.

[22] The only other data for comparison with our experimental observations we are aware of derive from field observations of the epiphytic leafy liverwort *Bazzania fauriana* in the subalpine forests of Taiwan [*Kao et al.*, 2000]. *Bazzania fauriana* was collected from branches of *Chamaecyparis* spp. and *Rhododendron formosum* at different heights of between 0.2 to 8 m above the forest floor, where they experienced a corresponding natural $[CO_2]_a$ gradient of ~30 ppm [*Kao et al.*, 2000]. In these forests, *B. fauriana* shows an increase in $\Delta^{13}C$ of 0.8‰ with the 30 ppm increase in CO_2, consistent with our results suggesting an increase of 0.7‰ over the same CO_2 range.

4.2. Sources of Natural $\Delta^{13}C$ Variation in Bryophytes

[23] Analysis across all species showed no significant difference in liverwort $\delta^{13}C$ between warm and cool sites (Table 4; Figure 2). However, there was a significant difference in $\delta^{13}C$ between individual liverwort species (ANOVA: $F = 62$, df = 3, $P < 0.001$), and between the way individual species responded to temperature ($F = 8$, df = 2, $P < 0.01$). Using the equations of *White et al.* [1994], a 4°C increase in temperature produces a 1.6 ‰ increase in $\delta^{13}C_p$ at 375 ppm. However, only one species in our temperature experiment showed a response consistent with this prediction and it is likely that differences in temperature optima between the species canceled specific temperature effects. This suggests it may be important to average across more than one species to minimize the effect of small temperature variations around the optimum growth temperature on $\delta^{13}C$ when inferring $[CO_2]_a$.

[24] No significant difference in $\delta^{13}C$ between growth substrates was found when all species were analyzed together. This result suggests no substantial photosynthetic uptake of soil-respired CO_2, which has a more negative

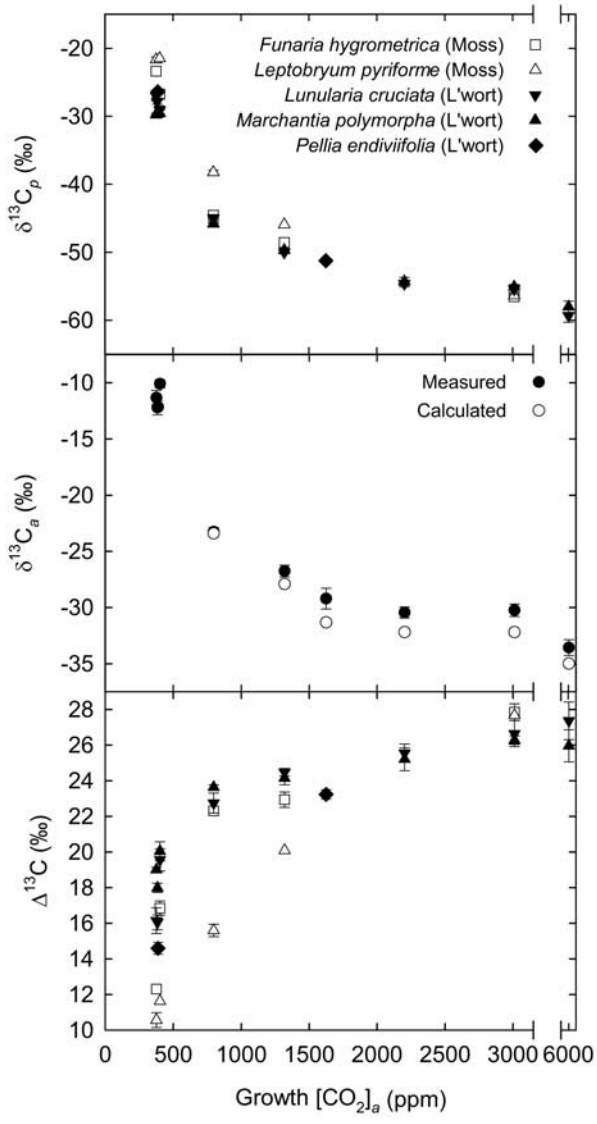

Figure 1. Effect of growth CO_2 concentration on (top) whole-tissue $\delta^{13}C$ of liverworts and mosses, (middle) the $\delta^{13}C_a$ of the air, and (bottom) bryophyte discrimination against ^{13}C ($\Delta^{13}C$).

Table 4. Carbon Isotope Composition of Liverworts Grown on Sand or Compost at Two Different Temperature Sites[a]

	$\delta^{13}C$, ‰			
	Cool Site		Warm Site	
Species	Sand Substrate	Compost Substrate	Sand Substrate	Compost Substrate
Conocephalum conicum	−26.83 ± 0.56	−27.20 ± 1.05	−28.11 ± 0.26	−27.37 ± 0.51
Lunularia cruciata	−29.23 ± 0.41	−28.76 ± 0.65	−29.42 ± 0.47	−29.89 ± 0.29
Marchantia polymorpha	−28.75 ± 0.23	−28.53 ± 0.19	−27.42 ± 0.03	−26.86 ± 0.14
Mean	−28.27	−28.16	−28.32	−28.04
Pellia epiphylla	−23.97 ± 0.96	−23.94 ± 0.37	did not grow	did not grow

[a]Data are ± standard error.

$\delta^{13}C$ than the atmospheric source [*Peterson and Fry*, 1987; *Sternberg et al.*, 1989], although in a dense forest understory with less turbulence and reduced air-mixing this effect could be more important [*Sternberg et al.*, 1989; *Kao et al.*, 2000].

[25] Water content affects bryophyte photosynthesis and $\Delta^{13}C$ more strongly than temperature [*Proctor et al.*, 1992; *White et al.*, 1994; *Rice and Giles*, 1996; *Williams and Flanagan*, 1996; *Rice*, 2000]. However, our field study of the long-term effect of habitat moisture regime (Table 2; Figure 3) showed no significant increases in either water content (1–5 g g^{-1} dry weight) or $\Delta^{13}C$ (0.04–0.6‰) for the liverworts at the wet sites (ANOVA: $F = 1$, df = 1, $P = 0.3$). The maintenance of high water content, 89–96%, in liverworts suggests that water storage is to an extent buffering variations in environmental conditions. In comparison, mosses showed larger and more variable increases in water content (13–32 g g^{-1} dry weight) at the wet sites (Table 2; Figure 3). Moreover, the increase in $\Delta^{13}C$ was also significantly larger (0.70–4.2‰) (ANOVA: $F = 58$, df = 1, $P < 0.001$) and more variable ($F = 20$, df = 2, $P < 0.001$). This $\Delta^{13}C$ increase contrasts with the results of on-line gas exchange studies showing that increased water content decreases $\Delta^{13}C$, as water films impose greater CO_2 diffusion-limitation on photosynthesis [*Rice and Giles*, 1996; *Williams and Flanagan*, 1996]. It nevertheless reinforces the idea that knowledge of past moss water content is important when inferring past $[CO_2]_a$ from them [*White et al.*, 1994; *Rice and Giles*, 1994].

[26] There was significant variation in $\delta^{13}C$ along the length of thallus of three liverworts (Table 5) (ANOVA: $F = 3$, df = 3, $P < 0.05$). Analysis across the three species showed that, because the patterns varied between species (Figure 4), overall both middle portions were quite different from the tip (Tukey multiple comparison test $P = 0.07$), and that overall the base was not different from the tip ($P = 0.64$). Variation along the thallus may be due to differences in the biochemical content of young and old material [*Damesin et al.*, 1998; *Hobbie et al.*, 2002]. The variation is less than that within other thallose photosynthetic organisms, such as brown algae and lichens, which can exhibit $\delta^{13}C$ differences within a thallus of up to 10‰ and 2.4‰, respectively [*Máguas and Brugnoli*, 1996; *Raven et al.*, 2002]. These results suggest that a reliable liverwort $\delta^{13}C$ estimate requires sampling from the same position of the thallus, or a minimum of three fossil species if the sampling position is not standardized.

[27] Comparison of measurements from the field and glasshouse studies with the growth chamber experiments shows that there was no growth chamber effect on $\Delta^{13}C$. The mean $\Delta^{13}C$ for *Marchantia* and *Lunularia* in ambient CO_2 experiments was 18.1‰, and for the field and glasshouse studies 18.5‰.

4.3. Modeling Bryophyte $\Delta^{13}C$ Responses to Atmospheric CO_2 Change

[28] We used our observations from the CO_2 experiments to develop a revised and extended isotopic fractionation model for bryophytes to better describe the dependency of $\Delta^{13}C$ on atmospheric CO_2 and predict past CO_2 concentrations. Our model development focuses on liverworts (with and without pores) because moss $\Delta^{13}C$ is strongly influenced by water availability (Figure 3) [*Rice and Giles*, 1996; *Williams and Flanagan*, 1996; *Rice*, 2000]. We begin by calculating ($[CO_2]_a - [CO_2]_i$) for both liverwort species across the range of $[CO_2]_a$ values used in our experiments, from measurements of $\delta^{13}C_p$ and $\delta^{13}C_a$ (Figure 1; Table 1), as given by equation (6) (Figure 5, top). Over the experimental $[CO_2]_a$ range, liverwort ($[CO_2]_a - [CO_2]_i$) is, as expected, an approximately linear

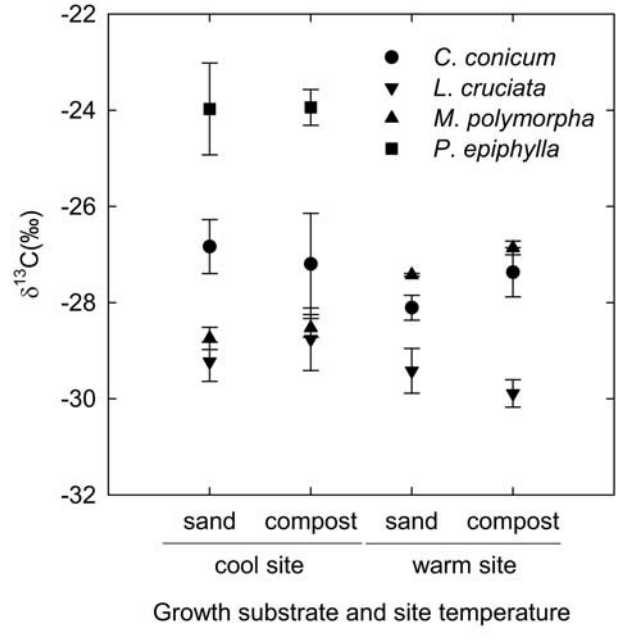

Figure 2. Effect of growth on sandy or peaty substrate in sites with two different temperatures on liverwort $\delta^{13}C$. Data are ± standard error.

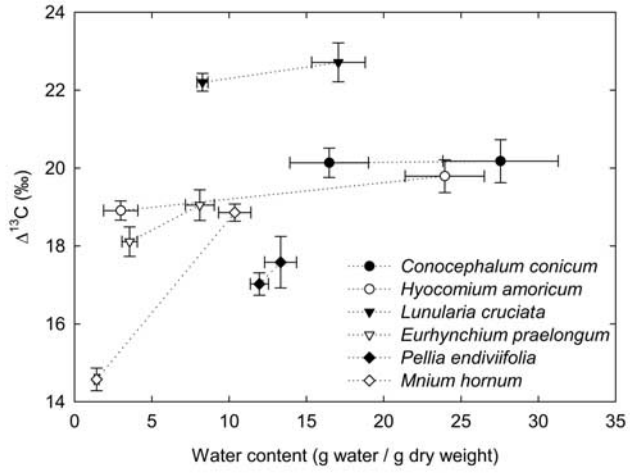

Figure 3. Discrimination against ^{13}C ($\Delta^{13}C$) of mosses (open symbols) and liverworts (solid symbols) in neighboring wet and dry patches. Plants were collected from wet and dry areas of a stone wall (circles), ditch bank (triangles), and cliff (diamonds). Wet and dry patch data are joined by dotted lines for ease of interpretation only. Data are ± standard error.

function of growth $[CO_2]_a$ ($F = 202$, df = 1,16, $P < 0.001$, $r^2 = 0.95$),

$$\left([CO_2]_a - [CO_2]_i\right)_{fit} = 130.61 + \left(0.1553 \cdot [CO_2]_a\right). \quad (10)$$

[29] Equation (10) implies A continues to increase up to 6000 ppm in agreement with earlier independent experiments on *Marchantia* [*Hanson et al.*, 2002]. To provide a further check on the physiological properties of the plants implied by our approach, we used equation (4), and an observed value of r (168 m^2 s mol^{-1} CO_2 for *Marchantia*) [*Green and Snelgar*, 1982, 1983], to calculate values of A at 400 ppm CO_2. This procedure yielded an A value of 1.2 μmol m^{-2} s^{-1}, close to but lower than a published estimate of ~2.0 μmol m^{-2} s^{-1} at ambient CO_2 [*Smith and Griffiths*, 2000; *Hanson et al.*, 2002; *Griffiths et al.*, 2004]. The lower calculated value may reflect the short-term nature of the direct photosynthesis measurements made under optimal conditions, or a lower value of r [*Proctor*, 1981]. Independent agreement in inferred A rates suggests that our model and experimental data accurately captures key aspects of liverwort physiology.

Table 5. Variation in $\delta^{13}C$ Along the Length of Liverwort Thalli[a]

Thallus quarter	$\delta^{13}C$ of Thallus Quarter, ‰			
	Conocephalum conicum	*Lunularia cruciata*	*Marchantia polymorpha*	Mean
Tip	−30.73 ± 0.62	−28.31 ± 0.35	−29.63 ± 0.40	−29.6
Mid-tip	−32.38 ± 0.09	−29.09 ± 0.39	−29.68 ± 0.30	−30.4
Mid-base	−32.23 ± 0.32	−29.62 ± 0.44	−29.29 ± 0.34	−30.4
Base	−31.42 ± 0.99	−29.48 ± 0.21	−28.94 ± 0.20	−29.9
Average	**−31.69 ± 0.44**	**−29.12 ± 0.34**	**−29.38 ± 0.20**	

[a]Data are ± standard error.

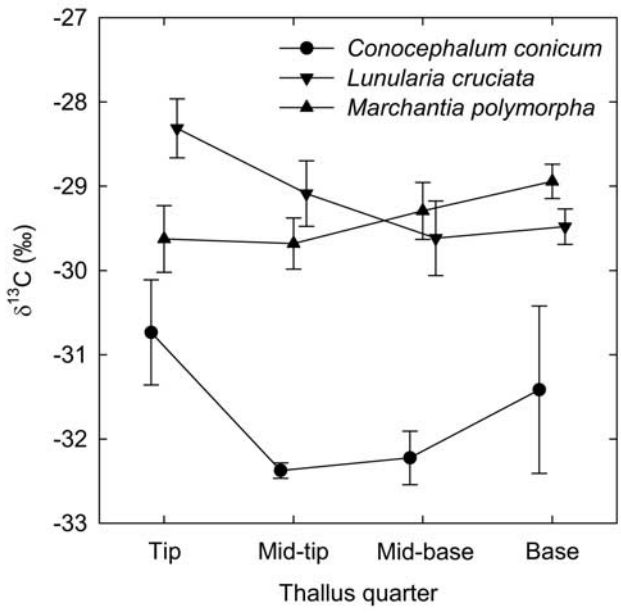

Figure 4. Variation in $\delta^{13}C_p$ along the length of liverwort thalli. Five individuals of three species with large thalli were divided into four equal pieces and the $\delta^{13}C$ determined: *Conocephalum conicum* (squares, full length 7–8 cm), *Lunularia cruciata* (point-down triangle, 3–4 cm), and *Marchantia polymorpha* (point-up triangle, 5–6 cm). Data are ± standard error.

[30] The mathematical outcome (equation (3)) of the rate of increase in $[CO_2]_a - [CO_2]_i$ over the CO_2 levels used in our experiments is an increase in $[CO_2]_i/[CO_2]_a$ as CO_2 rises, as a diminishing proportion of the atmospheric CO_2 is depleted inside the plants (Figure 5, middle, left axis). Equations (9) and (10) then define a curve accurately fitting the liverwort $\Delta^{13}C$ response data (Figure 5, bottom).

[31] Earlier work [*White et al.*, 1994; *Figge and White*, 1995] derived a $[CO_2]_a - [CO_2]_i$ response to $[CO_2]_a$ from separate measurements including A at sub-ambient $[CO_2]_a$ suggesting $[CO_2]_i/[CO_2]_a$ decreased as $[CO_2]_a$ rose leading to a fall in $\Delta^{13}C$. Whether this occurs depends on when the $[CO_2]_a - [CO_2]_i$ response curves at low $[CO_2]_a$ to point toward $[CO_2]_a - [CO_2]_i$ less than 0 (net respiration); for *Marchantia* this is below 200 ppm [*Smith and Griffiths*, 2000]. Accurately determining the $\Delta^{13}C$ response at low $[CO_2]_a$ requires growth experiments with bryophytes at sub-ambient $[CO_2]_a$.

4.4. Model Sensitivity

[32] We examined the sensitivity of the model to changes in the four physiological parameters which could vary owing to environmental and genotypic effects and influence the response of $\Delta^{13}C$ to $[CO_2]_a$. We assume the biochemical parameters a, b, e and f are constant between different plant species. The four key variables are: respiration rates (controlled by two variables), the sensitivity of photosynthesis to CO_2, and resistance to CO_2 diffusion.

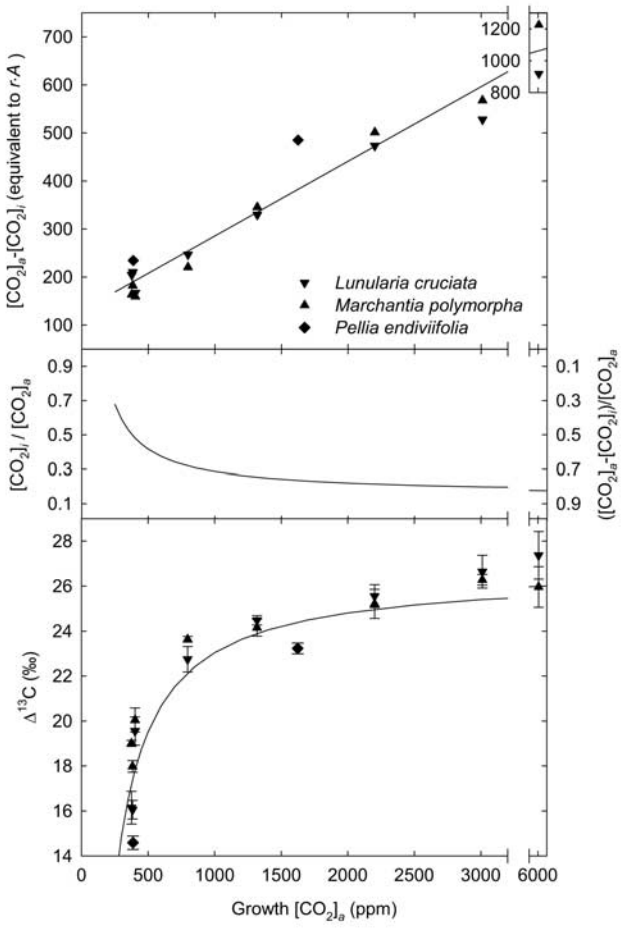

Figure 5. Calibration of the model of liverwort $\Delta^{13}C$ dependency on atmospheric CO_2. The difference between external and internal CO_2 was calculated from $\Delta^{13}C$ data for two species of liverwort: *Lunularia cruciata* (point-down triangle), *Marchantia polymorpha* (point-up triangle), and *Pellia endiviifolia* (squares), grown at a range of CO_2 levels, and a linear regression applied (top, line). From this the response of the $[CO_2]_i/[CO_2]_a$ ratio to CO_2 could be calculated (middle, line), allowing $\Delta^{13}C$ to be described as a function of CO_2 (bottom, line).

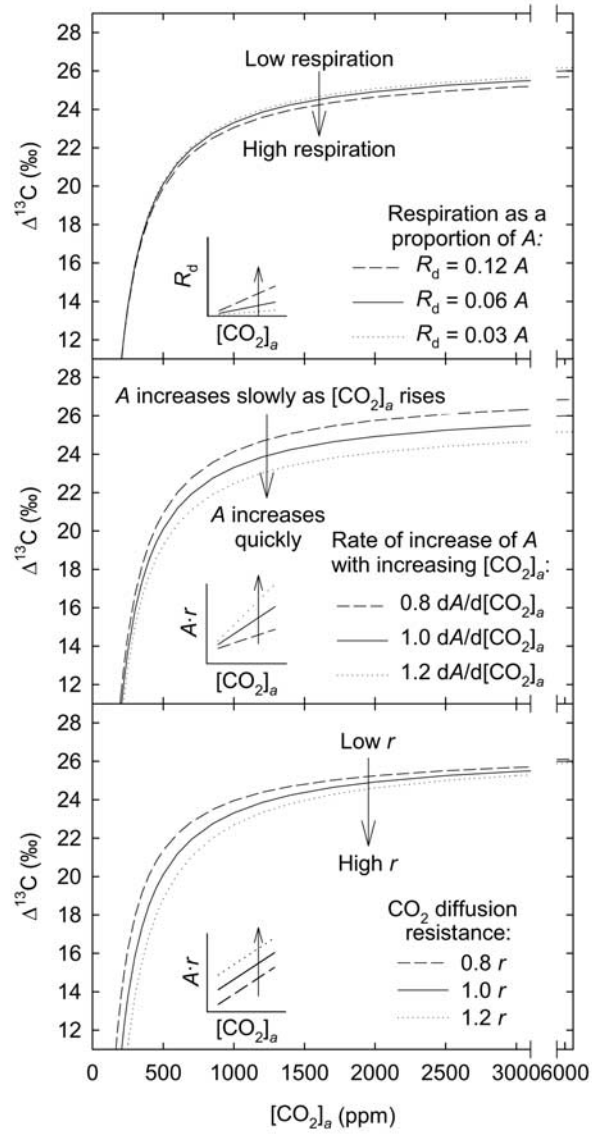

Figure 6. Sensitivity of modeled liverwort $\Delta^{13}C$ to changes in environmental and physiological variables. The subplots illustrate the physiological changes in relation to CO_2 driving the $\Delta^{13}C$ response, with arrows corresponding to the main plots. Three parameters of the model fit to experimental data (solid lines) were changed. (top) Dark respiration, $\times 2$ (dashed line) and $\times 0.5$ (dotted line); subplot illustrates the change in respiration as $[CO_2]_a$ increases. (middle) Rate of increase of photosynthesis with increasing CO_2 $\times 0.8$ (dashed line) and $\times 1.2$ (dotted line); subplot illustrates change in (photosynthesis x respiration) in a CO_2-dependant manner as $[CO_2]_a$ increases. (bottom) Resistance to CO_2 diffusion $\times 0.8$ (dashed line) and $\times 1.2$ (dotted line); subplot illustrates change in (photosynthesis $\times$ respiration) in a CO_2-independent manner as $[CO_2]_a$ increases; compare with middle panel subplot.

[33] In the model, changes in respiration rate are controlled (1) by the effect of temperature on the compensation point [*Brooks and Farquhar*, 1985] with an effect of <0.05‰ and (2) by the proportion of fixed carbon that is respired, initially set at 6%. Doubling the respiration rate decreases $\Delta^{13}C$ by 0.14‰ at 350 ppm and by slightly more at higher $[CO_2]_a$; halving it decreases $\Delta^{13}C$ by half this amount (Figure 6, top). As this is equivalent to an increase or decrease of 8–10°C [*Williams and Flanagan*, 1998], it is clear changes in respiration rate have only small effects on $\delta^{13}C$.

[34] Changes in the long-term A and r may be CO_2-dependant (the rate at which assimilation increases with CO_2, $dA/d[CO_2]_a$, or the rate at which resistance changes with CO_2), or CO_2-independent (other limitations). $dA/d[CO_2]_a$

(Figure 6, middle, subplot) is equivalent to the slope in Figure 5 (m in equation (7)). An increase of 20% reduces $\Delta^{13}C$ by 0.8‰, and vice versa (Figure 6, middle). $dA/d[CO_2]_a$ could be increased by adaptive thickening of the cuticle, or a reduction in the number of pores of Marchantalean liverworts, as CO_2 increases, although we know of no data describing this. $dA/d[CO_2]_a$ could be decreased by reducing Rubisco levels as CO_2 increased, but further data are required to assess this possibility.

[35] CO_2-independent limitations on r or A (Figure 6, bottom, subplot) are calculated as changes to the y-intercept in Figure 5, top (c in equation (7)); note that as $r \cdot A$ may not continue in a straight line at $[CO_2]_a$ below our measurements to actually intercept this point, it has no specific physiological meaning. The effect of increasing r is most marked at low $[CO_2]_a$. A 20% increase in r decreases $\Delta^{13}C$ by 2.0‰ at 350 ppm, 1.0‰ at 700 ppm, and 0.5‰ at 1400 ppm CO_2. This produces a steeper $\Delta^{13}C$ response curve that flattens out quickly at low r, and a shallower curve at high r (Figure 6, bottom). A may be affected by changes in factors such as light, temperature, water content, and possibly pH and nutrients, as well as $[CO_2]_a$ [*White et al.*, 1994, and references therein], and r is affected by changes in anatomy, water content and wind speed. However, bryophyte A saturates at relatively low light levels [*Green and Snelgar*, 1982; *Williams and Flanagan*, 1998; *Marschall and Proctor*, 2004], and has a fairly broad temperature optimum; for example, a 20% decrease in A is roughly equivalent to a halving of light from 200 to 100 μmol m^{-2} s^{-1} in *M. polymorpha* [*Marschall and Proctor*, 2004], or an increase or decrease of 10 °C from the optimum in temperate mosses [*Silvola*, 1985; *Williams and Flanagan*, 1998]. Bryophyte r is dominated by the boundary layer resistance [*Proctor*, 1982], and so small changes in thallus properties over time are unlikely to greatly influence r. This gives us confidence that the physiological response of liverworts to CO_2 can be determined robustly for use as a predictor of past atmospheric CO_2 concentrations.

4.5. Cretaceous Fossil Liverwort $\delta^{13}C$ and Paleo-CO_2 Estimates

[36] We analyzed the $\delta^{13}C$ composition of fossilized Cretaceous liverwort specimens to investigate the possibility indicated by our experimental observations that they record past CO_2 concentrations. The average $\delta^{13}C$ across all measurements was −26.5 ‰, which after adjusting for diagenesis [*Fletcher et al.*, 2004] and $\delta^{13}C_a$ gave an average $\Delta^{13}C$ of 23.4 ‰ (Table 3). Estimated using equation (8), the different liverwort genera yielded atmospheric CO_2 concentrations of 1514 ppm for *Marchantites* spp., 1382 ppm for *Thallites bicostatus*, and 1105 ppm for other liverworts. We obtained a mean value of 1334 ppm from an average of all three estimates. A possible source of error in liverwort estimations of past CO_2 concentrations is uncertainty in the $\delta^{13}C_a$, with a 1 ‰ error in its estimation roughly equivalent to a 1‰ error in $\Delta^{13}C$; at 1334 ppm, $\delta^{13}C_a \pm 0.5$‰ equates to a $[CO_2]_a$ error ∼+330 and −220 ppm. Overall, these results are in good general agreement with CO_2 estimates for this period based on stomatal and phytoplankton CO_2 proxies and are within the range of predictions by geochemical models [*Royer et al.*, 2004; *Berner and Kothavala*, 2001; *Bergman et al.*, 2004] (Figure 7).

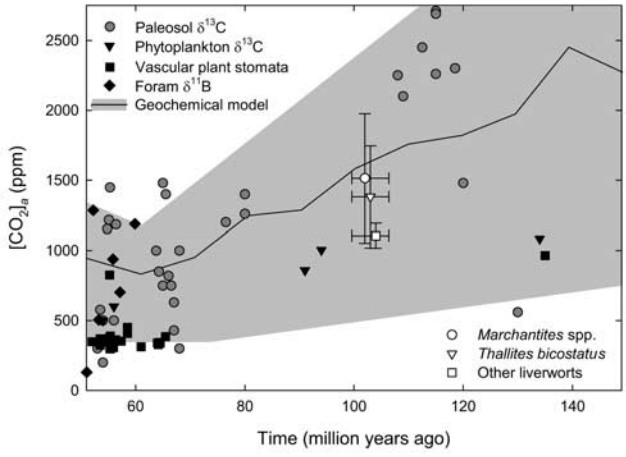

Figure 7. Comparison of atmospheric CO_2 estimated from Cretaceous liverworts and other sources. ^{13}C discrimination of the fossil liverworts *Marchantites arcuatus*, *M. pinnatus*, and *M. rosulatus* (open circles, $n = 4$); *Thallites bicostatus* (open triangle, $n = 3$) and other, unspecified liverworts (open square, $n = 8$) was used to estimate CO_2. Other paleo-CO_2 proxies for the period estimate CO_2 from the $\delta^{13}C$ of paleosol carbonates (shaded circle), $\delta^{13}C$ of phytoplankton (solid triangle), $\delta^{11}B$ of foraminifera (solid diamond), or vascular plant stomatal density (solid square). Line indicates atmospheric CO_2 predictions by the GEOCARB model of the long-term carbon cycle, region of uncertainty indicated by shaded areas [*Berner and Kothavala*, 2001]. Standard errors are shown for liverwort data only.

[37] In comparison with the fossil measurements, modern thallose liverworts growing in the Sheffield region have an average $\Delta^{13}C$ of 18.3 ‰ (four measurements on four species) [*Fletcher et al.*, 2004], which gives a CO_2 estimate (equation (8)) of 425 ppm, a value reasonably close to the modern $[CO_2]_a$ of 375 ppm [*Keeling and Whorf*, 2004]. Other measurements made on extant thallose liverworts show an average $\delta^{13}C$ of −29.2 ‰ (four measurements on four species) [*Proctor et al.*, 1992] and −27.4 ‰ (eight measurements on five species) [*Smith and Griffiths*, 1996a, 1996b], giving $\Delta^{13}C$ values of 21.9 ‰ and 19.9 ‰ when using global flask measurements of $\delta^{13}C_a$ [*Feng*, 1998], and CO_2 estimates of 777 and 532 ppm. In this case, it is possible that the flask measurements of $\delta^{13}C_a$ made at Pacific island research stations (i.e., Mauna Loa) may not be representative of the actual values of CO_2 assimilated by the liverworts studied near urban areas.

5. Conclusion

[38] Our results from two independent experimental systems consistently indicate that liverwort and moss $\Delta^{13}C$

increases sensitively in response to atmospheric CO_2 enrichment to levels above ambient. We have documented an ~8‰ increase in $\Delta^{13}C$ between ambient (375 ppm) and 6000 ppm CO_2, in a manner consistent with physiological models and marine phytoplankton, whose photosynthesis is also diffusion-limited as they too lack waxy cuticles or stomata. Other environmental factors, including temperature, substrate availability and spatial heterogeneity produce far smaller responses than the effect of CO_2 and can be greatly minimized by averaging across a number of different species. Our case study of Cretaceous fossil liverworts yielded atmospheric CO_2 concentrations consistent with other CO_2 proxies and indicates they hold great promise as a new means of reconstructing the CO_2 content of the ancient atmosphere.

[39] We note that some molecular [*Qiu et al.*, 1998] and morphological [*Wellman et al.*, 2003] evidence suggests that the earliest land plants were of liverwort-like affinity. These simple plants operated without stomata, or at least probably without functional stomata, and must have been dependent upon simple diffusion for CO_2 uptake. Modern bryophytes therefore may provide a reasonable physiological and functional analogue for their ancestral forms. If this analogy is correct, our results point to the possibility that the fossilized remains of early land plants (mesofossils and spores), which are abundant in Ordovician and Silurian sediments, retain a quantitative atmospheric CO_2 signature. Recovering this signal would offer a CO_2 proxy with the capacity to reach back to the Ordovician and provide important constraints on the predictions of long-term carbon cycle models for that time.

Notation

a ^{13}C fractionation due to molecular diffusion effects (4.4‰).

A photosynthetic assimilation rate, μmol CO_2 m^{-2} s^{-1}.

b ^{13}C fractionation due to photosynthesis effects (30‰).

c offset in linear regression of $(r \cdot A)$ against $[CO_2]_a$, ppm.

$[CO_2]_a$ atmospheric CO_2 concentration in the air outside the leaf or thallus (ppm = μmol CO_2 mol^{-1} gas).

$[CO_2]_i$ intercellular CO_2 concentration within leaf or thallus (ppm = μmol CO_2 mol^{-1} gas).

e ^{13}C fractionation due to dark respiration effects (7‰).

f ^{13}C fractionation due to photorespiration effects (2‰).

g $0.06 \cdot e/(1 + 0.06)$ a factor removed to simplify the equations, ‰.

k $(A + R_d)/(C_i - \Gamma_*) = (1 + 0.06)A/(C_i - \Gamma_*)$ (mol m^{-2} s^{-1}), where $R_d = 0.06A$.

m slope in linear regression of $([CO_2]_a - [CO_2]_i)$ against $[CO_2]_a$, ppm ppm^{-1}.

r total resistance to diffusion of CO_2 from outside the leaf or thallus to the site of photosynthesis (m^2 s mol^{-1}). In non-molar units 1 m^2 s mol^{-1} = 44.6 s m^{-1} for an ideal gas at STP.

R_d rate of dark respiration, $0.06A$, μmol CO_2 m^{-2} s^{-1}.

$\delta^{13}C_a$ stable carbon isotope composition of atmospheric CO_2, ‰.

$\delta^{13}C_p$ stable carbon isotope composition of plant material, ‰.

Γ_* CO_2 compensation point for photorespiration versus carboxylation; a quadratic function of temperature given by *Brooks and Farquhar* [1985].

[40] **Acknowledgments.** We thank Alistair Crame at the British Antarctic Survey for providing access to the Cretaceous fossil liverworts for isotopic analysis, Paul Koch and Paul Quick for helpful discussion and comment on the manuscript, and Heather Walker for technical expertise. B. J. F. gratefully acknowledges funding from a University of Sheffield studentship. S. J. B. was funded through an NERC award to D. J. B. (NER/A/S/2001/00435).

References

Beerling, D. J., and D. L. Royer (2002), Fossil plants as indicators of the Phanerozoic global carbon cycle, *Annu. Rev. Earth Planet. Sci.*, *153*, 387–397.

Beerling, D. J., F. I. Woodward, M. R. Lomas, M. A. Wills, W. P. Quick, and P. J. Valdes (1998), The influence of Carboniferous palaeoatmospheres on plant function: An experimental and modelling assessment, *Philos. Trans. R. Soc. London, Ser. B*, *353*, 131–139.

Beerling, D. J., J. A. Lake, R. A. Berner, L. J. Hickey, D. W. Taylor, and D. L. Royer (2002), Carbon isotope evidence implying high O_2/CO_2 ratios in the Permo-Carboniferous atmosphere, *Geochim. Cosmochim. Acta*, *66*, 3757–3767.

Bergman, N. M., T. M. Lenton, and A. J. Watson (2004), COPSE: A new model of biogeochemical cycling over Phanerozoic time, *Am. J. Sci.*, *304*, 397–437.

Berner, R. A. (2004), *The Phanerozoic Carbon Cycle: CO_2 and O_2*, Oxford Univ. Press, New York.

Berner, R. A., and Z. Kothavala (2001), Geocarb III: A revised model of atmospheric CO_2 over Phanerozoic time, *Am. J. Sci.*, *301*, 182–204.

Brooks, A., and G. D. Farquhar (1985), Effect of temperature on the CO_2-O_2 specificity of ribulose-1,5- biphosphate carboxylase/oxygenase and the rate of respiration in the light: Estimates from gas exchange measurements on spinach, *Planta*, *165*, 397–406.

Cantrill, D. J. (1997), Hepatophytes from the early Cretaceous of Alexander Island, Antarctica: Systematics and paleoecology, *Int. J. Plant Sci.*, *158*, 476–488.

Cerling, T. E. (1991), Carbon dioxide in the atmosphere: Evidence from Cenozoic and Mesozoic paleosols, *Am. J. Sci.*, *291*, 377–400.

Cowan, I. R. (1977), Stomatal behaviour and environment, *Adv. Bot. Res.*, *4*, 117–227.

Crowley, T. J., and R. A. Berner (2001), CO_2 and climate change, *Science*, *292*, 870–872.

Damesin, C., S. Rambal, and R. Joffre (1998), Seasonal and annual changes in leaf $\delta^{13}C$ in two co-occurring Mediterranean oaks: Relations to leaf growth and drought progression, *Funct. Ecol.*, *12*, 778–785.

Farquhar, G. D., and J. Lloyd (1993), Carbon and oxygen isotope effects in the exchange of carbon dioxide between terrestrial plants and the atmosphere, in *Stable Isotopes and Plant Carbon-Water Relations*, edited by J. R. Ehleringer, A. E. Hall, and G. D. Farquhar, pp. 47–70, Elsevier, New York.

Farquhar, G. D., M. H. O'Leary, and J. A. Berry (1982), On the relationship between carbon isotope discrimination and the intercellular carbon dioxide concentration in leaves, *Aust. J. Plant Physiol.*, *9*, 121–137.

Farquhar, G. D., J. R. Ehleringer, and K. T. Hubick (1989), Carbon isotope discrimination and photosynthesis, *Annu. Rev. Plant Phys. Plant Mol. Biol.*, *40*, 503–537.

Feng, X. (1998), Long-term c_i/c_a response of trees in western North America to atmospheric CO_2 concentration derived from carbon isotope chronologies, *Oecologia*, *117*, 19–25.

Figge, R. A., and J. W. C. White (1995), High-resolution Holocene and late glacial atmospheric CO_2 record: Variability tied to changes in thermohaline circulation, *Global Biogeochem. Cycles*, *9*, 391–403.

Fletcher, B. J., D. J. Beerling, and W. G. Chaloner (2004), Stable carbon isotopes and the metabolism of the terrestrial Devonian organism *Spongiophyton*, *Geobiology*, *2*, 107–119.

Freeman, K. H., and J. M. Hayes (1992), Fractionation of carbon isotopes by phyto-plankton and estimates of ancient CO_2 levels, *Global Biogeochem. Cycles*, *6*, 185–198.

Giordano, M., J. Beardall, and J. A. Raven (2005), CO_2 concentrating mechanisms in algae: Mechanisms, environmental modulation, and evolution, *Annu. Rev. Plant Biol.*, *56*, 99–131.

Gradstein, F., J. Ogg, and A. Smith (2004), *A Geologic Time Scale 2004*, 589 pp., Cambridge Univ. Press, New York.

Green, T. G. A., and W. P. Snelgar (1982), A comparison of photosynthesis in two thalloid liverworts, *Oecologia*, *54*, 275–280.

Green, T. G. A., and W. P. Snelgar (1983), Erratum: A comparison of photosynthesis in two thalloid liverworts, *Oecologia*, *57*, 420.

Griffiths, H., K. Maxwell, D. Richardson, and W. Robe (2004), Turning the land green: Inferring photosynthetic physiology and diffusive limitations in early bryophytes, in *The Evolution of Plant Physiology From Whole Plants to Ecosystems*, edited by A. R. Hemsley and I. Poole, pp. 3–16, Elsevier, New York.

Hanson, D., T. J. Andrews, and M. R. Badger (2002), Variability of the pyrenoid-based CO_2 concentrating mechanism in hornworts (Anthocerotophyta), *Funct. Plant Biol.*, *29*, 407–416.

Hobbie, E. A., J. Gregg, D. M. Olszyk, P. T. Rygiewicz, and D. T. Tingey (2002), Effect of climate change on labile and structural carbon in Douglas-fir needles as estimated by $\delta^{13}C$ and C_{area} measurements, *Global Change Biol.*, *8*, 1072–1084.

Kao, W.-Y., Y.-S. Chiu, and W.-H. Chen (2000), Vertical profiles of CO_2 concentration and $\delta^{13}C$ values in a subalpine forest of Taiwan, *Bot. Bull. Acad. Sin.*, *41*, 213–218.

Kashiwagi, H., and N. Shikazono (2003), Climate change during Cenozoic inferred from global carbon cycle model including igneous and hydrothermal activities, *Palaeogeogr. Palaeoclimatol. Palaeoecol.*, *199*, 167–185.

Keeling, C. D., and T. P. Whorf (2004), Atmospheric CO_2 records from sites in the SIO air sampling network, in *Trends*: *A Compendium of Data on Global Change*, pp. 16–26, Carbon Dioxide Inf. Anal. Cent., Oak Ridge Natl. Lab., U.S. Dep. of Energy, Oak Ridge, Tenn. (Available at cdiac.esd.ornl.gov/trends/co2/sio-keel.htm)

Kelly, S. R. S., and A. C. M. Moncreiff (1992), Marine molluscan constraints on the age of Cretaceous forests of Alexander Island, Antarctica, *Geol. Mag.*, *129*, 771–778.

Laws, E. A., B. N. Popp, R. R. Bidigare, M. C. Kennicut, and S. A. Macko (1995), Dependence of phytoplankton carbon isotope composition on growth rate and $[CO_2]_{aq}$: Theoretical considerations and experimental results, *Geochim. Cosmochim. Acta*, *59*, 1131–1138.

Laws, E. A., B. N. Popp, N. Cassar, and J. Tanimoto (2002), ^{13}C discrimination patterns in oceanic phytoplankton: Likely influence of CO_2 concentrating mechanisms, and implications for palaeoreconstructions, *Funct. Plant Biol.*, *29*, 323–333.

MacLeod, K. G., B. T. Huber, and M. Le Ducharme (2000), Paleontological and geochemical constraints on changes in the deep ocean during the Cretaceous greenhouse interval, in *Warm Climates in Earth History*, edited by B. Huber, K. MacLeod, and S. Wing, pp. 241–274, Cambridge Univ. Press, New York.

Máguas, C., and E. Brugnoli (1996), Spatial variation in carbon isotope discrimination across the thalli of several lichen species, *Plant Cell Environ.*, *19*, 437–446.

Marschall, M., and M. C. Proctor (2004), Are bryophytes shade plants? Photosynthetic light responses and proportions of chlorophyll *a*, chlorophyll *b* and total carotenoids, *Ann. Bot.*, *94*, 593–603.

McElwain, J. C., and W. G. Chaloner (1995), Stomatal density and index of fossil plants track atmospheric carbon dioxide in the Paleozoic, *Ann. Bot.*, *76*, 389–395.

Moncreiff, A. C. M., and S. R. S. Kelly (1993), Lithostratigraphy of the uppermost Fossil Bluff Group (Early Cretaceous) of Alexander Island, Antarctica: History of an Albian regression, *Cretaceous Res.*, *14*, 1–15.

Mook, W. G. (1986), C in atmospheric CO_2, *Neth. J. Sea Res.*, *20*, 211–223.

Mook, W. G., J. C. Bommerson, and W. H. Staverman (1974), Carbon isotope fractionation between dissolved bicarbonate and gaseous carbon dioxide, *Earth Planet. Sci. Lett.*, *22*, 169–176.

Mora, C. I., S. G. Driese, and L. A. Colarusso (1996), Middle to late Palaeozoic atmospheric CO_2 levels from soil carbonate and organic matter, *Science*, *271*, 1105–1107.

Oostendorp, C. (1987), *The Bryophytes of the Palaeozoic and Mesozoic*, J. Cramer, Berlin.

Pagani, M., M. A. Arthur, and K. H. Freeman (1999), Miocene evolution of atmospheric carbon dioxide, *Paleoceanography*, *14*, 273–292.

Pearson, P. N., and M. R. Palmer (2000), Atmospheric carbon dioxide concentrations over the past 60 million years, *Nature*, *406*, 695–699.

Peterson, B. J., and B. Fry (1987), Stable isotopes in ecosystem studies, *Annu. Rev. Ecol. Syst.*, *18*, 293–320.

Popp, B. N., E. A. Laws, R. R. Bidigare, J. E. Dore, K. L. Hanson, and S. G. Wakeham (1998), Effect of phytoplankton cell geometry on carbon isotopic fractionation, *Geochim. Cosmochim. Acta*, *62*, 69–77.

Proctor, M. C. F. (1981), Diffusion resistances in bryophytes, in *Plants and Their Atmospheric Environment*, edited by J. Grace, E. D. Ford, and P. G. Jarvis, pp. 219–229, Blackwell Sci., Malden, Mass.

Proctor, M. C. F. (1982), Physiological ecology: Water relations, light and temperature responses, carbon balance, in *Bryophyte Ecology*, edited by A. J. E. Smith, pp. 333–382, CRC, Boca Raton, Fla.

Proctor, M. C. F., J. A. R. Raven, and S. K. Rice (1992), Stable carbon isotope discrimination measurements in *Sphagnum* and other bryophytes: Physiological and ecological implications, *J. Bryol.*, *17*, 193–202.

Qiu, Y.-L., C. Yangrae, J. C. Cox, and J. Palmer (1998), The gain of three mitochondrial introns identifies liverworts as the earliest land plants, *Nature*, *394*, 671–674.

Raven, J. A. (2002), Selection pressures on stomatal evolution, *New Phytol.*, *153*, 371–386.

Raven, J. A., et al. (2002), Mechanistic interpretation of carbon isotope discrimination by marine macroalgae and seagrasses, *Funct. Plant Biol.*, *29, 355–378.*

Raven, P. H., R. F. Evert, and S. E. Eichhorn (1999), *Biology of Plants*, 6th ed., W. H. Freeman, New York.

Rice, S. K. (2000), Variation in carbon isotope discrimination within and among Sphagnum species in a temperate wetland, *Oecologia*, *123*, 1–8.

Rice, S. K., and L. Giles (1994), Climate in the Pleistocene, *Nature*, *371*, 111.

Rice, S. K., and L. Giles (1996), The influence of water content and leaf anatomy on carbon isotopic discrimination and photosynthesis in *Sphagnum*, *Plant Cell Environ.*, *19*, 118–124.

Royer, D. L., R. A. Berner, and D. J. Beerling (2001a), Phanerozoic CO_2 change: Evaluating geochemical and paleobiological approaches, *Earth Sci. Rev.*, *54*, 349–392.

Royer, D. L., S. L. Wing, D. J. Beerling, D. W. Jolley, P. L. Koch, L. J. Hickey, and R. A. Berner (2001b), Paleobotanical evidence for near present-day levels of atmospheric CO_2 during part of the Tertiary, *Science*, *292*, 2310–2313.

Royer, D. L., R. A. Berner, I. P. Montañez, N. J. Tabor, and D. J. Beerling (2004), CO_2 as a primary driver of Phanerozoic climate, *GSA Today*, *14*(3), 4–10.

Shaw, J., and K. Renzaglia (2004), Phylogeny and diversification of bryophytes, *Am. J. Bot.*, *91*, 1557–1581.

Silvola, J. (1985), CO_2 dependence of photosynthesis in certain forest mosses and peat mosses and simulated photosynthesis at various actual and hypothetical CO_2 concentrations, *Lindbergia*, *11*, 86–93.

Smith, A. G., D. G. Smith, and B. M. Funnell (1994), *Atlas of Mesozoic and Cenozoic coastlines*, Cambridge Univ. Press, New York.

Smith, E. C., and H. Griffiths (1996a), The occurrence of the chloroplast pyrenoid is correlated with the activity of a CO_2-concentrating mechanism and carbon isotope discrimination in lichens and bryophytes, *Planta*, *198*, 6–16.

Smith, E. C., and H. Griffiths (1996b), A pyrenoid-based carbon-concentrating mechanism is present in terrestrial bryophytes of the class Anthocerotae, *Planta*, *200*, 203–212.

Smith, E. C., and H. Griffiths (2000), The role of carbonic anhydrase in photosynthesis and the activity of the carbon-concentrating-mechanism in bryophytes of the class Anthocerotae, *New Phytol.*, *145*, 29–37.

Sternberg, L. D. L., S. S. Mulkey, and S. J. Wright (1989), Ecological interpretation of leaf carbon isotope ratios: Influence of respired carbon dioxide, *Ecology*, *70*, 1317–1324.

Tajika, E. (1998), Climate change during the last 150 million years: reconstruction from a carbon cycle model, *Earth Planet. Sci. Lett.*, *160*, 695–707.

Van der Burgh, J., H. Visscher, D. L. Dilcher, and W. M. Kürschner (1993), Paleoatmospheric signatures in Neogene fossil leaves, *Science*, *260*, 1788–1790.

Veizer, J., et al. (1999), $^{87}Sr/^{86}Sr$, $\delta^{13}C$ and $\delta^{18}O$ evolution of Phanerozoic seawater, *Chem. Geol.*, *161*, 59–88.

Veizer, J., Y. Godderis, and L. M. Francois (2000), Evidence for decoupling of atmospheric CO_2 and global climate during the Phanerozoic eon, *Nature*, *408*, 698–701.

Wallmann, K. (2001), Controls on the Cretaceous and Cenozoic evolution of seawater composition, atmospheric CO_2 and climate, *Geochim. Cosmochim. Acta*, *65*, 3005–3025.

Wellman, C. H., P. L. Osterloff, and U. Mohiuddin (2003), Fragments of the earliest land plants, *Nature*, *425*, 282–285.

White, J. W. C., R. A. Figge, P. Ciais, V. Markgraf, and R. Kenny (1994), Climate in the Pleistocene, *Nature*, *371*, 111–112.

Williams, T. G., and L. B. Flanagan (1996), Effect of water content on photosynthesis, transpiration and discrimination against $^{13}CO_2$ and $C^{18}O^{16}O$ in *Pleurozium* and *Sphagnum*, *Oecologia*, *108*, 38–46.

Williams, T. G., and L. B. Flanagan (1998), Measuring and modelling environmental influences on photosynthetic gas exchange in *Sphagnum* and *Pleurozium*, *Plant Cell Environ.*, *21*, 555–564.

Yapp, C. J., and H. Poths (1992), Ancient atmospheric CO_2 pressures inferred from natural goethites, *Nature*, *355*, 342–344.

D. J. Beerling, S. J. Brentnall, and B. J. Fletcher, Department of Animal and Plant Sciences, University of Sheffield, Alfred Denny Building, Western Bank, Sheffield S10 2TN, UK. (d.j.beerling@sheffield.ac.uk)

D. L. Royer, Department of Earth and Environmental Sciences, Wesleyan University, 265 Church Street, Middletown, CT 06459-0139, USA.